Annals of Agri-Bio Research **29** (1): 23-29, 2024

Impact Score : 0.28 (Scopus)

Green Synthesis, Characterization and Stability Analysis of ZnO Nanoparticles Doped with Different Cu Concentrations

BAHAREH DABAGHIANNEJAD*, SANDEEP KUMAR ARYA AND SANDEEP KUMAR[1]

Department of Electronics and Communication Engineering, Guru Jambheshwar University of Science and Technology, Hisar-125 001 (Haryana), India
**(e-mail: b.dabaghian@gmail.com; Mobile: 97297 66137)*

(Received: September 7, 2023; Accepted: November 10, 2023)

ABSTRACT

In this study, zinc oxide (ZnO) nanoparticles doped with copper (Cu) at different concentrations were synthesized via green synthesis using lime juice. The ZnO formation was confirmed through the X-ray diffraction (XRD) analysis in all samples and crystallite sizes between 32 and 52 nm were obtained. Adding Cu and increasing its concentration caused a blue shift in the UV absorption of the samples and the band gap energy increased from 3.3 to 4 eV. The images obtained from the Field Emission Scanning Electron Microscopy (FESEM) and morphological studies showed the change in the shape of nanoparticles from flake-shaped for pure ZnO to irregular-shaped for doped ones. However, the growth of grains was of the nano range and size of the produced particles was smaller than 60 nm. The Fourier-Transform Infrared spectroscopy (FTIR) study of the samples also proved the presence of zinc oxide. Observing peaks at 3416 to 3447/cm showed the presence of moisture in nano-powders. Finally, the results from zeta potential characterization showed a good stability of nanoparticles in colloidal at lower pH proving the role of citric acid available in the lime juice to enhance the stability and prevent sediment. The optical and band gap properties of the nanoparticles were engineered by the addition of different concentrations of Cu and the stability of the materials was improved by the change of the pH of the solution.

Key words: Green synthesis, ZnO, Cu-doped ZnO, UV-Vis, band gap energy, zeta potential

INTRODUCTION

Since the advent of nanotechnology, various materials have been developed in nano sizes for a variety of purposes. The main feature of these materials that changes or increases their application is having a larger surface area compared to their bulk forms. This seemingly small difference plays a huge role in changing the physical and chemical properties of the produced materials. Zinc oxide (ZnO) is one of the materials that have caught a lot of attention in nano form. Due to its unique physical and chemical properties, this material has found its place in a wide range of applications, including paint, ceramics, medicine, food and electronics. At room temperature, ZnO has an energy band gap of 3.36 eV and exciton energy of 60 meV, both of which make it a very suitable option for use in optoelectronics, photovoltaic cells, solar cells, optoelectronic devices such as LEDs and other electromagnetic applications. One of the characteristics of many nanoscale metal oxides is that they are good hosts for impurities, meaning that they are well receptive to impurities within their crystal lattice. The presence of impurities in the host crystal often causes changes in the properties of the material. Depending on the desired properties, the materials selected for doping vary; for example, adding iron (Fe) to ZnO improves its electromagnetic properties by changing the band gap (Ciciliati *et al.*, 2015) and introducing copper (Cu) in ZnO crystals boosts its optical properties (Karimi *et al.*, 2017). Also studies have shown that the addition of transition metals to the structure of zinc oxide has resulted in favourable changes for different applications (Karmakar *et al.*, 2018). One of the important and influential factors on the properties of nanomaterials is their shape and size. Different studies have synthesized ZnO in the forms of nano-flakes (Singh and Soni, 2020), nano-belts (Hong *et al.*, 2021), nano-rods (Khalid *et al.*, 2019), nano-wires (Manzano *et*

[1]Physics Department, Punjab Engineering College (Deemed to be University), Sector 12, Chandigarh-160 012 (Chandigarh), India.

al., 2022) and flower-shaped (Bishwakarma *et al.*, 2023). These morphologies and in what size they are obtained strongly depend on how they are synthesized. Among methods used to make ZnO nanoparticles, hydrothermal (Gerbreders *et al.*, 2020), chemical vapor deposition (Zhao *et al.*, 2016), physical vapor deposition (Mohammed *et al.*, 2020) can be mentioned. Among the properties of nanomaterials, electrochemical properties play a significant role when stability of the material especially in colloid form is important. In 2018, Shinohara *et al.* (2018) studied the effect of citric acid on the stability of hafnium oxide and showed improvement in the zeta potential of the prepared nanoparticles. In this study, the facile co-precipitation green synthesis for doping zinc oxide was worked with copper to study the effect of natural citric acid and the concentration of the introduced impurities on the properties of zinc oxide.

MATERIALS AND METHODS

Limes were purchased from the vegetable market. All the chemicals used were as received without further purifications. Zinc Acetate Dihydrate (M.W. 219.50), Copper (II) Acetate Monohydrate (M.W. 199.65), Polyvinyl Pyrrolidone K-25 (Povidone, PVP) (M.W.~10000), Sodium Hydroxide (NaOH, M.W. 40) and Double Distilled Water (DDW) were used in the sets of experiments.

The lime juice was extracted manually and then filtered using Whatman filter to remove pulps. The pH of the juice was 3 before starting the experiments. To dope zinc nanoparticles with copper at different concentrations four experiments were conducted as follow. A solution of 2.2 g zinc acetate in 50 mllime juice was prepared followed by the addition of 0.01, 0.04, 0.07 and 0.1 M copper acetate. Thus, four different concentrations of copper were added to the solution of zinc salt and lime juice, while the concentration of zinc oxide was kept constant. Each solution was stirred for 10 min until a homogeneous solution was obtained. Polyvinyl Pyrrolidone K-25 was used as the capping agent to prevent the further agglomeration of the nanoparticles and for that 1 g of PVP was dissolved in 50 ml DDW and stirred until a transparent solution appeared. The solution of PVP was added drop-wise to the solution of salts and dopants under vigorous stirring. A fresh solution of 0.4 g NaOH in 50 ml DDW was then added drop by drop to the above solutions as the reducing agent to complete the reactions mean while the pH of the solution was measured until it reached 8. The solutions were kept stirring overnight and then transferred to the sonication bath for 2 h. To remove the ionic impurities, the samples were washed multiple times with distilled water and two times with ethanol and finally dried at 70°C overnight. The samples were then crushed for 15 min and stored for further use. To prepare ZnO nanoparticles the aforementioned steps were followed exactly the same without the addition of dopants.

The X-Ray diffraction analysis of all samples was performed using Rigaku Multiflex-II with CuKα radiation (λ=1.5406 A°). The morphological and surface properties as well as the average particle size analysis were done by a JEOL brand, model JSM, 7610 FPLUS Schottky Field Emission SEM (FESEM). To investigate the optical properties of the samples Shimadzu UV2450 UV-Vis spectrometer was used. The Fourier Transform Infrared (FTIR) analysis was obtained from a PerkinElmer Spectrum IR Version 10.6.2. The zeta potential studies were done using Malvern Zetasizer Nano ZS size analyzer.

RESULTS AND DISCUSSION

In order to find out the internal atomic structure of the produced materials, the XRD was run. The data obtained for pure zinc oxide represented the hexagonal Wurtzite structure which was completely in agreement with the ICDD file as shown in Table 1.

Table 1. XRD peaks of ZnO from ICDD file and peaks obtained from the experiment

XRD peak	2θ degree from ICDD	2θ degree of ZnO
1 0 0	31.770	31.74
0 0 2	34.422	34.42
1 0 1	36.253	36.26
1 0 2	47.539	47.46
1 1 0	56.603	56.58

When Cu is doped in zinc oxide, the Cu^{2+} ions are placed into the ZnO crystal in two ways: either they replace Zn^{2+} ions, or they are placed in the inner space between Zn and oxygen ions (Karimi *et al.*, 2017). Since copper ions have a

smaller size (smaller diameter) than zinc ions, they do not change ZnO crystal structure by being substituted in its crystal. In addition, according if the amount of copper is less than 15%, it does not cause any special change in the crystalline of ZnO and its shape is preserved. However, if the concentration of copper increases the crystal structure undergoes a change. The results of the XRD analysis are shown in Fig. 1 and it is clearly visible that 100, 002 and 101 peaks were influenced with the Cu concentration. Increasing the amount of the dopant caused a reduction in the sharpness of peaks that were characteristic of zinc oxide and proved the sitting of Cu ions inside the ZnO crystallite (Fig. 1).

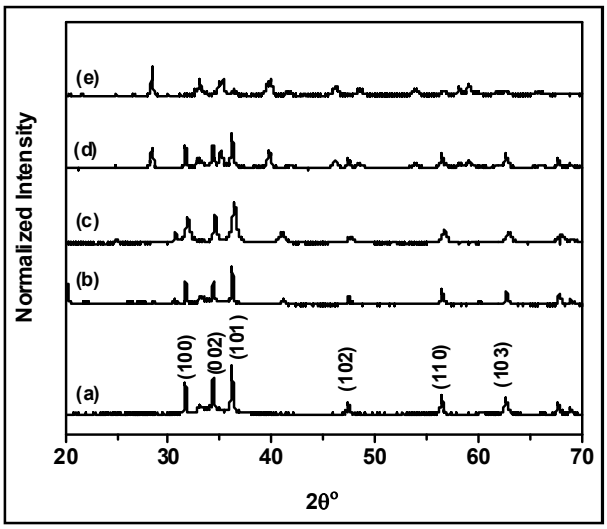

Fig. 1. XRD analysis of (a) pure ZnO, (b) 0.01 M Cu doped ZnO, (c) 0.04 M Cu doped ZnO, (d) 0.07 M Cu doped ZnO and (e) 0.1 M Cu doped ZnO.

Crystallite size (*L*) of all samples was computed using Debye-Scherrer formula with putting the XRD data in the equation 1:

$$L = \frac{k\lambda}{\beta \cos \theta} \quad ...(1)$$

Where, λ (the X-ray wavelength) was almost equal to 1.54 ° A, β was the full width half Maxima in radian (FWHM), θ was the peak position, and depending on the size of the crystallite *k* was a constant from 0.62 to 2.08, which was 0.94 in this study. According to the calculations, the average size of the pure ZnO crystal was estimated to be 39.8 nm, and the size of the crystal doped with 0.01 M Cu was found to be 32.9 nm, which indicated the presence of Cu^{2+} ions with a smaller diameter in the zinc oxide crystal. As the concentration of Cu^{2+} ions increased the crystallite size gradually increased and reached 34.8, 45.6 and finally 52.3 nm for 0.04, 0.07 and 0.1 M Cu doped ZnO.

The optical properties of un-doped and doped ZnO with different concentrations of copper were studied by UV- Vis spectrum analysis. Using this characterization enables the study of UV absorption properties of the materials as a function of wavelength. All samples were dissolved in double distilled water with the ratio of 1 mg in 1 ml and sonicated for 1 h. The pure ZnO showed an absorption peak at 379 nm which was the reference of the comparison for the doped nanomaterials (Fig. 2). The introduction of a small amount of copper impurity to the zinc oxide crystal caused a blue shift and the occurrence of its peak at the wavelength of 359 nm. The shift in the absorption wavelength was directly related to the presence of Cu^{2+} ions in the zinc oxide crystal, which caused the change in the crystal structure of this material by substituting the Zn^{2+} ions or placing in the inner space of Zn and O ions. After that, the blue shift was repeated by adding impurity concentration. However, when its amount was increased to 0.07 M, in addition to the shift in the absorption peak, the range of absorbed wavelengths also broadened and nanoparticles absorbed wavelengths from 280 to 362 nm which covered a huge area of UVA (from 320 to

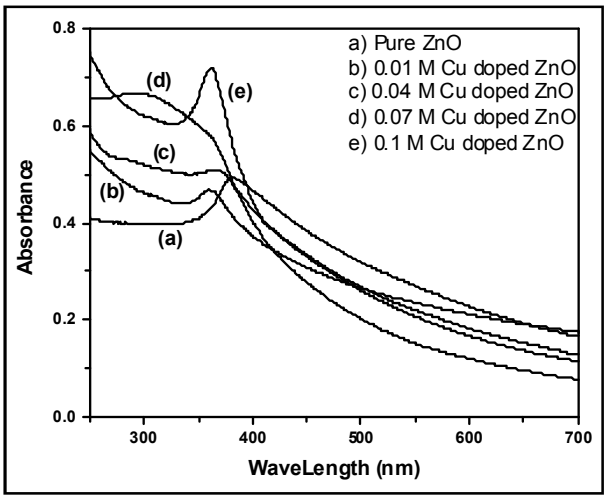

Fig. 2. UV-Vis spectroscopy of green synthesized pure ZnO and Cu-doped ZnO nanoparticles.

400 nm), all area of UVB (from 290 to 320 nm) and some area of UVC (from 100 to 290 nm). At the concentration of 0.1 M, the peak again occurred at a single wavelength of 362 nm. This showed the sensitivity of UV absorption to the amount of the dopant since adding to the dopant further did not lead to a wider range of absorption. Therefore, controlling the concentration of the impurities is of a great importance to reach to the point where most of the demands were fulfilled.

Using the data obtained from UV absorption and applying equation 2 and drawing the TAUC plots, the band gap energy of each sample was calculated separately as:

$$\alpha\nu = A\,(\nu - Eg)^{n} \qquad ...(2)$$

Where, α and h were the absorption coefficient and Planck's constant, respectively. A was a constant, ν was the energy of a photon and n indicated different transitions as 1/2 for permitted direct, 2 for permitted indirect, 3/2 for forbidden direct and 3 for forbidden indirect transition. Since ZnO was a semiconductor with permitted direct transition the equation 2 became the following:

$$\alpha\nu = A\,(\nu - Eg)^{1/2} \qquad ...(3)$$

The band gap of zinc oxide changed after the attendance of copper impurity (Fig. 3). The increase in band gap after doping could be clarified by the Burstein-Moss effect (Kadam *et al.*, 2017; Zhou *et al.*, 2023). The direct band gap of CuO was 1.85 eV and adding it to the zinc oxide caused an increase in the band gap. Yet again the importance of the amount of dopant can be seen in the size of the band gap. The FESEM was used to find information about the morphology and size of the produced particles (Fig. 4). Pure ZnO nanoparticles showed flake-shaped, and with the addition of Cu and increasing its concentration, the appearance of the particles became amorphous. The agglomeration of particles showed the grain growth in the range of nanometers. Particles doped with 0.01 M Cu had sizes of 40-60 nm with the average of 45 which was close to the average size of un-doped ZnO, but with the addition of impurities, the average particle size increased such as 55, 58 and 62 nm for 0.04, 0.07 and 0.1 M Cu doped, respectively.

Fourier Transform Infrared Spectroscopy was done for pure ZnO and Cu doped ZnO samples in order to gain information about the functional groups present in the crystal of nanoparticles and different absorption bands

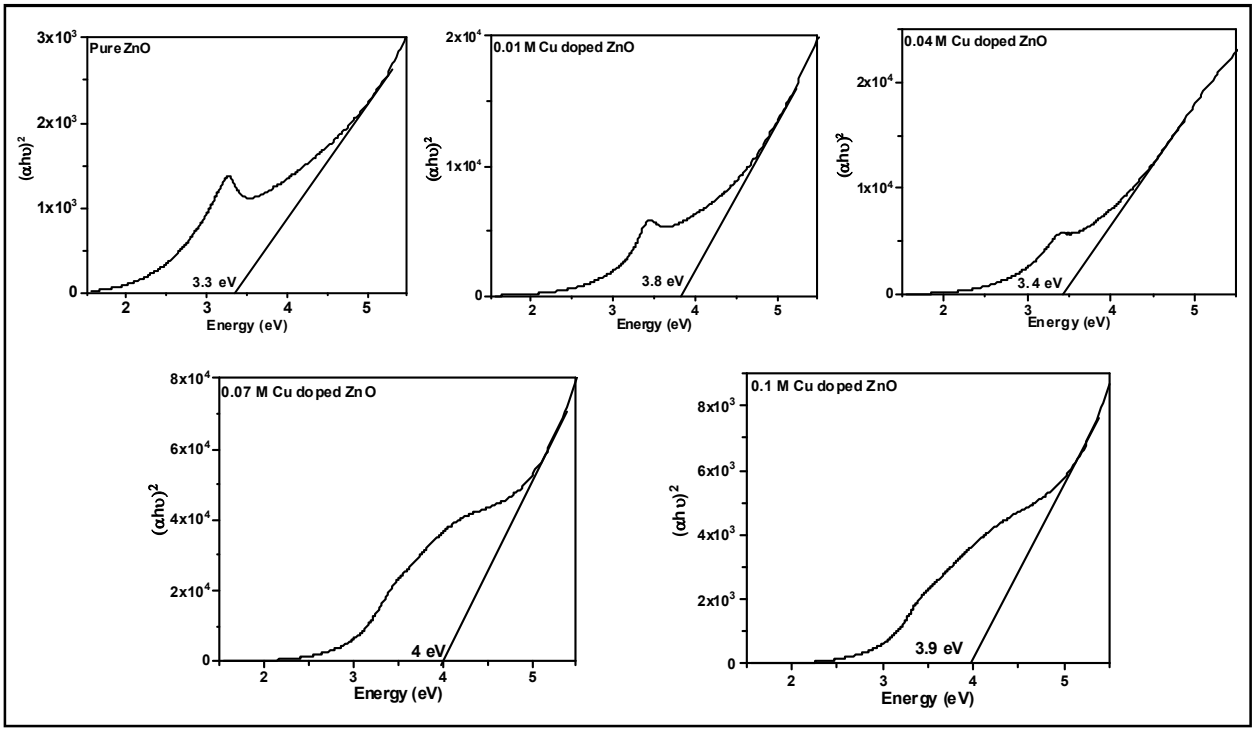

Fig. 3. Tauc plots of un-doped and doped ZnO and from UV-Vis Spectroscopy.

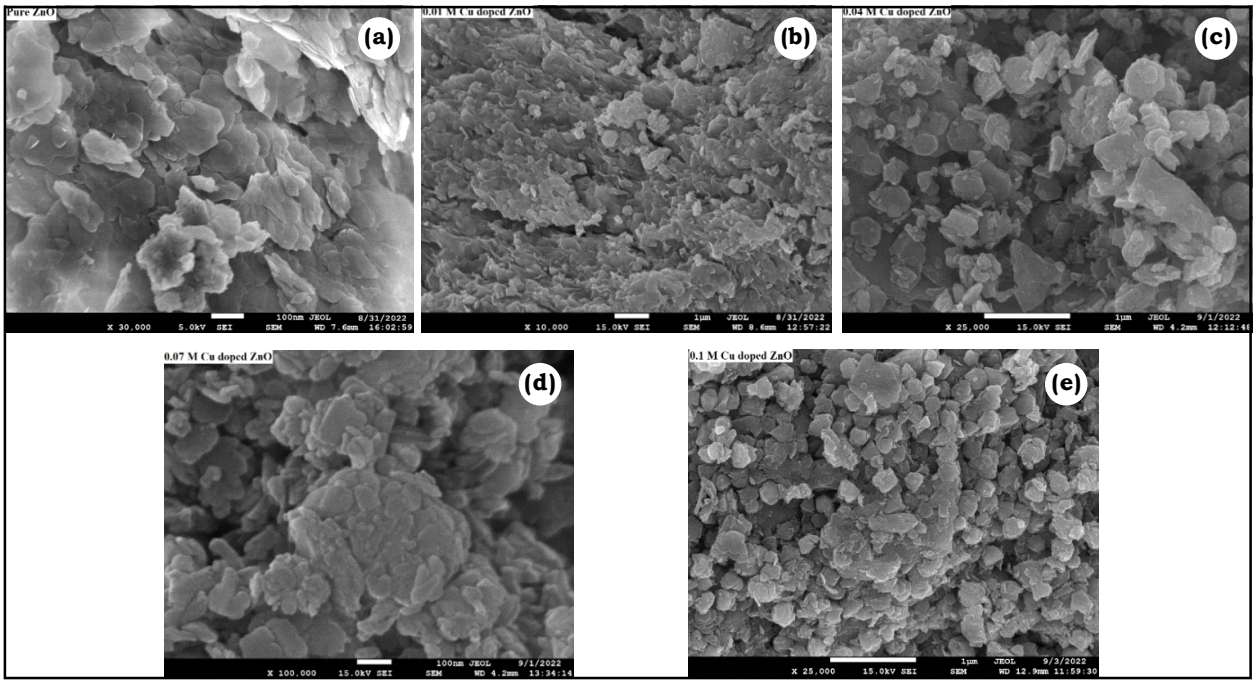

Fig. 4. SEM images of (a) pure ZnO, (b) 0.01 M Cu doped ZnO, (c) 0.04 M Cu doped ZnO, (d) 0.07 M Cu doped ZnO and (e) 0.1 M Cu doped ZnO.

were obtained (Fig. 5). In all samples, the peaks between 418 and 459/cm related to the stretching vibration of Zn-O bond indicated the formation of ZnO in all the samples. Peaks occurred between 600 to 674/cm in doped samples can be attributed to weak bonds of Zn-O stretching vibration which was due to the impurities of Cu. The absorption at 882/cm for pure ZnO was related to medium vibration of Zn-O which shifted in the case of doped samples. The region between 1022 and 1123/cm corresponded to the OH. The peaks occurring between 1344 and 1630/cm were representing the C-O and C-C bending vibration. Finally, the peaks between 3416 to 3447/cm were in agreement with the strong broad H-O stretching vibration which happened due to the absorbance of humidity by nanoparticles.

To obtain information about the electrochemical properties of the produced materials, the zeta potential of the materials was investigated using Zetasizer. Since ZnO is a versatile metal oxide used in various industries, its electrochemical properties such as stability in liquid is of special importance. For this characterization materials were dispersed in the solutions of water and water-lime juice with different pH and sonicated for one hour. The results showed a strong relation between the pH of the solution and the size and zeta potential.

Starting with water (pH=7.5) the sizes of the particles were close to the sizes obtained from SEM analysis and the zeta potential was measured (Table 2) where ZP referred to zeta potential. The particle size and the zeta potential were inversely related, meaning particles with bigger size (0.1 M Cu doped ZnO) showed lower zeta potential and therefore lower stability, whereas particles with smaller size (0.01 M Cu doped ZnO) had higher zeta potential and better stability.

By adding different concentration of lime juice and reaching to the pH of 7, 6.5 and 5.8, the best zeta potential results occurred at the lowest pH. In addition, by reducing the pH a reduction in the size of the nanoparticles was noticed (Fig. 6). The Cu-doped ZnO nanoparticles followed the similar pattern. This can be attributed to the citric acid present in lime juice which was absorbed by the nanoparticles creating a repulsive force between particles and preventing them from aggregation. The results are in a good agreement with DLVO theory (Abdelfatah *et al.*, 2017).

CONCLUSION

Using a simple and cost-effective method of co-precipitation and green synthesis using lime

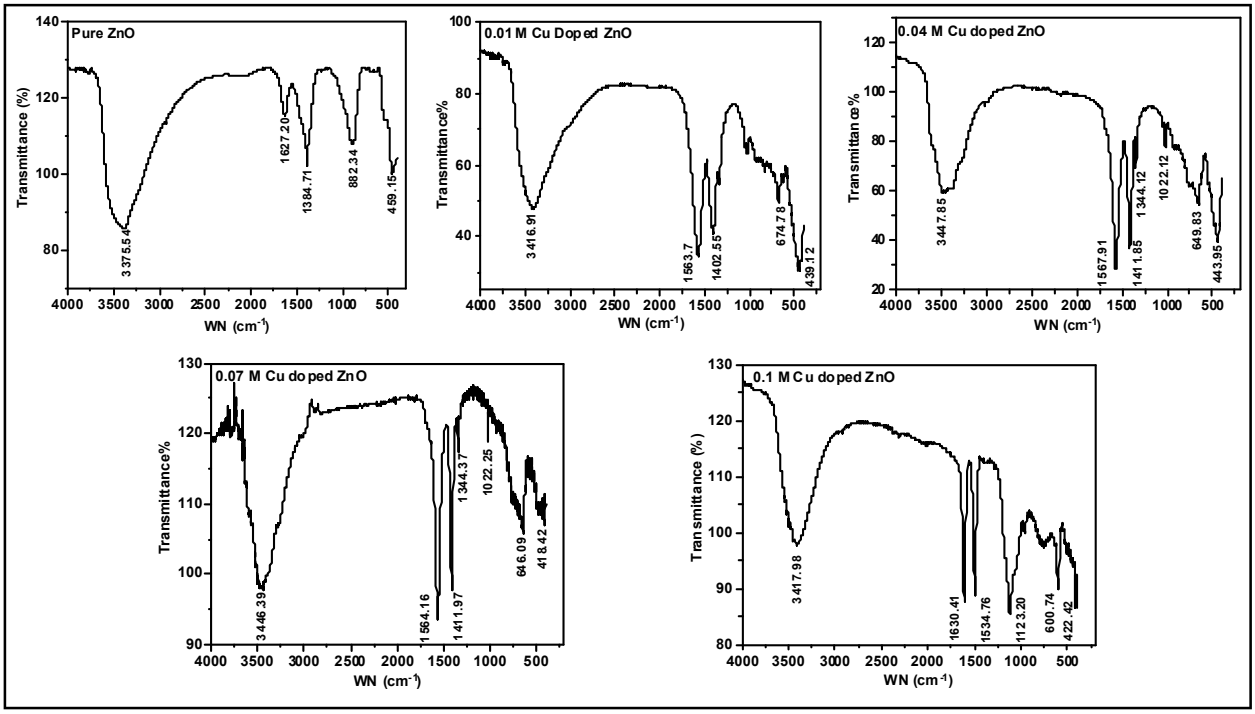

Fig. 5. FTIR spectra of pure and Cu-doped ZnO.

Table 2. Zeta potential of un-doped and Cu doped ZnO in different pH solutions

pH	ZP (mV) of 0.01 M Cu doped ZnO	ZP (mV) of 0.04 M Cu doped ZnO	ZP (mV) of 0.07 M Cu doped ZnO	ZP (mV) of 0.1 M Cu doped ZnO	ZP (mV) of pure ZnO
7.5	+20.2	+13.1	+11.2	+10	+15
7.0	-25.5	-17.2	-18.2	-15.6	-22.1
6.5	-29.3	-21	-20.1	-18	-28.3
5.8	-32.8	-22.9	-22.3	-21.7	-30.1

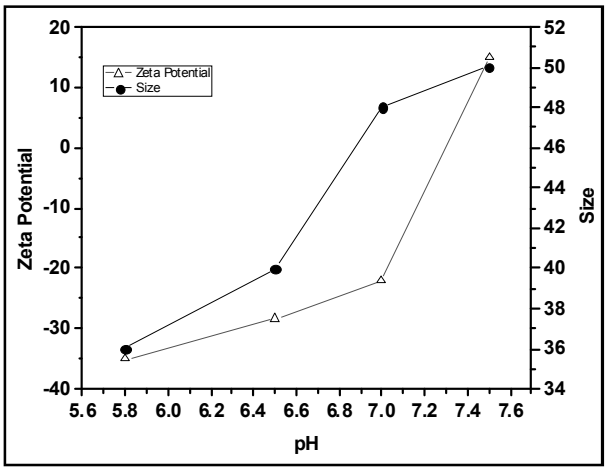

Fig. 6. The relation and effect of pH on the zeta potential and size of the pure ZnO nanoparticles.

juice, pristine zinc oxide and zinc oxide doped with copper were fabricated at concentrations of 0.01, 0.04, 0.07 and 0.1 M. For all samples XRD, FTIR, FESEM and UV-Vis characterizations were performed. Both XRD and FTIR proved the formation of zinc oxide in all samples. The crystallite size of the samples was calculated using Debye-Scherrer formula and the shrinking of the crystals of 0.01 M (32.9 nm) and 0.04 M (34.8 nm) samples compared to pure zinc oxide (39.8 nm) indicated the presence of Cu^{+2} ions with a smaller diameter than Zn^{+2} ions in the crystal of zinc oxide. In the FTIR analysis, in addition to the strong bonds of Zn-O, moisture and weak bonds of Zn-O were also observed, which indicated the absorption of water and settling of Cu^{+2} ions, respectively. The results obtained from FESEM showed that the presence of even a small amount of impurity to the ZnO affected the shape of the particles and changed them from flake to amorphous. But the growth of the particles was still in the nano range and the average size of the particles was smaller than 60 nm. In the UV-VIS analysis,

the UV absorption of the particles showed a blue shift from 379 nm after the introduction of the impurity, and at a concentration of 0.07 M, the wavelength of absorption became extensive 280-362 nm. Also, the band gap energy of doped particles increased compared to pure ZnO from 3.3 to 4 eV. Finally, the electrochemical properties of the materials were studied via zeta potential measurements in different pH solutions showing a relation between the pH and the zeta potential. As the pH decreased the zeta potential and so the stability of the materials in the solution increased. This study showed the significance of controlling the dopant concentration and the colloid pH to achieve the desired optical and electrochemical properties of the nanoparticles to enhance their application.

REFERENCES

Abdelfatah, E. R., Kang, K., Pournik, M., Shiau, B., Harwell, J., Haroun, M. R. and Rahman, M. M. (2017). Study of nanoparticle adsorption and release in porous media based on the DLVO theory. In: *SPE Latin Am. Caribbean Petro. Eng. Conf.* **2017.** *.https://doi.org/10.2118/185484-MS.*

Bishwakarma, H., Tyagi, R., Kumar, N. and Das, A. K. (2023). Green synthesis of flower shape ZnO-GO nanocomposite through optimized discharge parameter and its efficiency in energy storage device. *Environ. Res.* **218**: 115021. *https://doi.org/10.1016/j.envres.2022.115021.*

Ciciliati, M. A., Silva, M. F., Fernandes, D. M., DeMelo, M. A. C., Hechenleitner, A. A. W. and Pineda, E. A. G. (2015). Fe-doped ZnO nanoparticles: Synthesis by a modified Sol–Gel method and characterization. *Mat. Letters* **159**: 84-86. *https://doi.org/10.1016/j.matlet.2015.06.023.*

Gerbreders, V., Krasovska, M., Sledevskis, E., Gerbreders, A., Mihailova, I., Tamanis, E. and Ogurcovs, A. (2020). Hydrothermal synthesis of ZnO nanostructures with controllable morphology change. *Cryst. Eng. Comm.* **22**: 1346-1358. *doi: 10.1039/c9ce01556f.*

Hong, M., Meng, J., Yu, H., Du, J., Ou, Y., Liao, Q., Kang, Z., Zhang, Z. and Zhang, Y. (2021). Ultra-stable ZnO nanobelts in electrochemical environments. *Mat. Chem. Front.* **5**: 430-437.*https://doi.org/10.1039/D0QM00709A.*

Kadam, A. N., Kim, T. G., Shin, D. S., Garadkar, K. M. and Park, J. (2017). Morphological evolution of Cu doped ZnO for enhancement of photocatalytic activity. *J. Alloys Compounds* **710**: 102-13. *https://doi.org/10.1016/j.jallcom.2017.03.150.*

Karimi, M., Rastegar Ramsheh, M., Jodaeia, A., Ahmadi, S. M., Jahangir, V., Ghasemi, M. and Behhtaj Lejbini, M. (2017). Sonochemically synthesized ZnO and Zno.9CuO.1O nanoparticles as photocatalysts for MB optodecolorizatio. *Optoelectr. Adv. Mat.* **19**: 641-649.

Karmakar, S., Panda, B., Sahoo, B., Routray, K. L., Varma, S. and Behera, D. (2018). A study on optical and dielectric properties of Ni-ZnO nanocomposite. *Mat. Sci. Semicond. Proces.* **88**:198-206. *https://doi.org/10.1016/j.mssp.2018.08.008.*

Khalid, N. R., Hammad, A., Tahir, M. B., Rafique, M., Iqbal, T., Nabi, G. and Hussain, M. K. (2019). Enhanced photocatalytic activity of Al and Fe Co-doped ZnO nanorods for methylene blue degradation. *Ceram. Int.* **45**: 21430-21435. *https://doi.org/10.1016/j.ceramint.2019.07.132.*

Manzano, C. V., Philippe, L. and Serrà, A. (2022). Recent progress in the electrochemical deposition of ZnO nanowires: Synthesis approaches and applications. *Crit. Rev. Solid State Mat. Sci.* **47**: 772-805. *https://doi.org/10.1080/10408436.2021.1989663.*

Mohammed, R. Y., Sabah, A., Abdulrahman, A. and Hamad, S. (2020). Synthesis and characterizations of ZnO thin films grown by physical vapor deposition technique. *J. Appl. Sci. Tech. Tren.* **1**: 135-139. *doi: 10.38094/jastt1456.*

Shinohara, S., Eom, N., Teh, E. J., Tamad, K., Parsons, D. and Craig, V. S. J. (2018). The role of citric acid in the stabilization of nanoparticles and colloidal particles in the environment: Measurement of surface forces between hafnium oxide surfaces in the presence of citric acid. *Langmuir* **34**: 2595-2605. *doi: 10.1021/acs.langmuir.7b03116.*

Singh, J. and Soni, R. K. (2020). Controlled synthesis of CuO decorated defect enriched ZnO nanoflakes for improved sunlight-induced photocatalytic degradation of organic pollutants. *Appl. Surf. Sci.* **521**: 146420. *https://doi.org/10.1016/j.apsusc.2020.146420.*

Zhao, Y., Li, C., Chen, M., Yu, X., Chang, Y., Chen, A., Zhu, H. and Tang, Z. (2016). Growth of aligned ZnO nanowires via modified atmospheric pressure chemical vapor deposition. *Phy. Lett. A* **380**: 3993-3997. *https://doi.org/10.1016/j.physleta.2016.06.030.*

Zhou, X., Huang, E., Zhang, R., Xiang, H., Zhong, W. and Xu, B. (2023). Multicolour tunable electrochromic materials based on the burstein–moss effect. *Nanomat.* **13**: 1580. *https://doi.org/10.3390/nano13101580.*